Supporting Information

Regulation of nitrogen reduction reaction catalytic performance by varying sp/sp^2 hybrid carbon ratio in graphyne/graphene heterojunction catalysts

Zexiang Yin[1#], *Zijun Yang*[1#], *Yingmei Bian*[1], *Heng Zhao*[1], *Beijia Chen*[1], *Yuan Liu*[3], *Yang Wang*[1*], *Yida Deng*[1*], *Haozhi Wang*[1,2,4,5*]

[1] State Key Laboratory of Tropic Ocean Engineering Materials and Materials Evaluation, School of Materials Science and Engineering, School of Mechanical and Electrical Engineering, Hainan University, Haikou, 570228 China
[2] Key Laboratory of Pico Electron Microscopy of Hainan Province, School of Materials Science and Engineering, Hainan University, Haikou, 570228 China
[3] State Key Laboratory of Precious Metal Functional Materials, School of Materials Science and Engineering, Tianjin University, Tianjin, 300072 China
[4] Key Laboratory of Advanced Energy Materials Chemistry (Ministry of Education), Nankai University, Tianjin, 300071 China
[5] Key Laboratory of Computational Physical Sciences (Ministry of Education), Fudan University, Shanghai, 200433 China
#*Zexiang Yin* and *Zijun Yang* contributed equally to this work.

Computational Details

We used VASPKIT [Wang, V., Xu, N., Liu, J.-C., Tang, G. & Geng, W.-T. Comput. Phys. Commun., 108033 (2021).] to construct heterojunction models of graphyne and graphene, ensuring that the lattice mismatch was kept below 5%. The models were selected based on the criteria that the benzene rings of graphyne and graphene are as aligned as possible, with a lattice pinch angle of 60° or 90°, and the total number of atoms in the structure does not exceed 200.

All computations were conducted using the Vienna Ab initio Simulation Package (VASP) with

spin-polarized first-principles method [1,2]. The projector augmented-wave (PAW) approach was employed to describe both core and valence electrons. The generalized gradient approximation (GGA) in the Perdew-Burke-Ernzerhof (PBE) form was used to characterize the electron-core interaction and exchange-correlation functions [3–5]. Electronic wave functions were expanded using a plane-wave basis with a kinetic energy cutoff of 400 eV. A 2×2×1 TM@GY supercell was utilized for the simulations, and a 15 Å vacuum layer was introduced vertically to the basal plane of the TM@GY supercell to mitigate spurious interlayer interactions. For geometric optimizations, a 2×2×1 Γ-centered Gamma scheme k-mesh was employed to sample the first Brillouin zone. The total energy convergence was set to 10^{-5}. The relaxation of all atoms was continued until the force acting on each atom was less than 0.01 eV/Å. To account for long-range van der Waals interactions, the DFT-D3 method was used [6,7]. To investigate the stability of TM@GY, ab initio molecular dynamics (AIMD) simulations were conducted based on the geometry-optimized results. The Nose heat bath was utilized to maintain a temperature of 300 K, with a time step of 1 fs. The total simulation time was set to 5 ps to achieve a thermodynamically balanced state.

The binding energy (E_b) of the TM atom supported on GY is determined by the equation:

$$E_b = E_{TM@GY} - E_{GY} - E_{TM} \quad (1)$$

where $E_{TM@GY}$ represents the total energy of the TM atom supported on GY, and E_{GY} and E_{TM} correspond to the energies of GY and a single TM atom, respectively.

The Gibbs free energy change (ΔG) for individual hydrogenation steps in the nitrogen reduction reaction (NRR) process was determined using the computational hydrogen electrode (CHE) model as proposed by Nørskov and collaborators. [8,9]. The values of ΔG for each step in the NRR were calculated using the following equation.:

$$\Delta G = \Delta E_{DFT} + \Delta E_{ZPE} - T\Delta S + \Delta G_U + \Delta G_{pH} \quad (2)$$

where ΔE_{DFT} is the variation in electronic energy before and after the hydrogenation, directly determined through DFT calculations. ΔE_{ZPE} and ΔS denote the zero-point energy correction and entropy alteration, respectively, derived from frequency calculations at 298.15 K [10]. ΔG_U accounts for the contribution of the applied electrode potential (U) to ΔG, while ΔG_{pH} corrects for the free energy change due to H^+.

The Gibbs free energy of the adsorption of *NNH intermediates on the catalysts is expressed as:

$$\Delta G_{*NNH} = \Delta G_{TM@GY + *NNH} - \Delta G_{TM@GY} - \Delta G_{NNH} \quad (3)$$

where ΔG_{NNH} is determined as the sum of the Gibbs free energies of N_2 and $1/2H_2$ molecules:

$$\Delta G_{NNH} = \Delta G_{N_2} + 1/2\Delta G_{H_2} \quad (4)$$

In these equations, $\Delta G_{TM@GY + NNH*}$ and $\Delta G_{TM@GY}$ represent the total Gibbs free energy of NNH species adsorbed on TM@GY, while ΔG_{N2} and ΔG_{H2} are the Gibbs free energies of N_2 and H_2 molecules, respectively. A similar approach is used to calculate the Gibbs free energy of other intermediates.

The Gibbs free energy barrier between two intermediates, such as between *NNH and $*N_2$, is expressed as $\Delta G_{*NNH - *N2}$:

$$\Delta G_{*NNH - *N2} = \Delta G_{*NNH} - \Delta G_{*N_2} \quad (5)$$

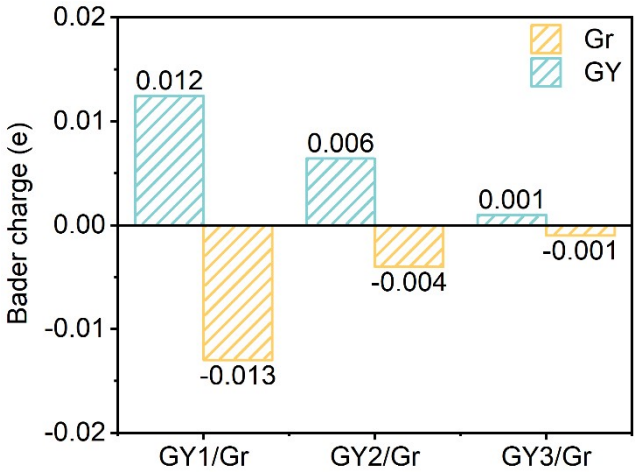

Fig. S1 The average value of the Bader charge projected onto each atom of GY and Gr in the GY/Gr.

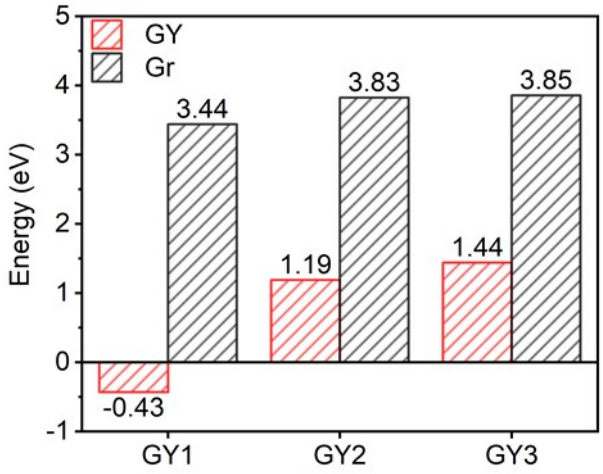

Fig. S2 Ti adsorption energy on GY and Gr.

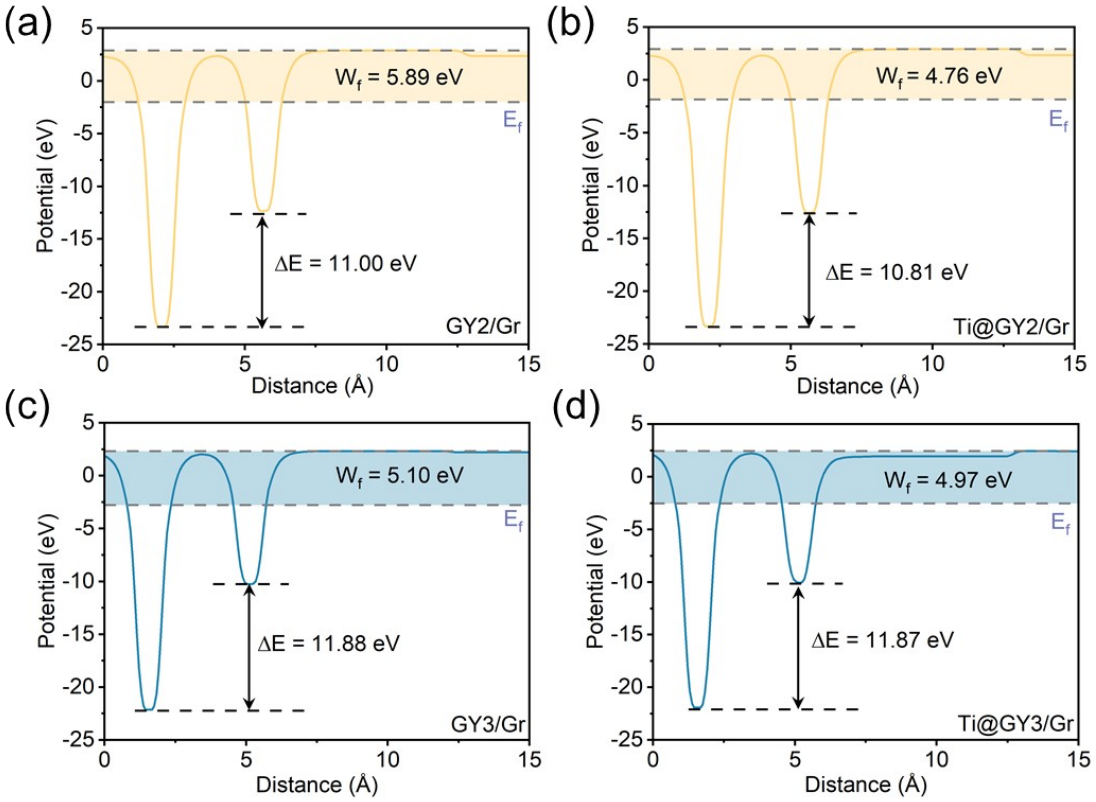

Fig. S3 (a-d) The work function of GY2/Gr, Ti@GY2/Gr, GY3/Gr and Ti@GY3/Gr respectively.

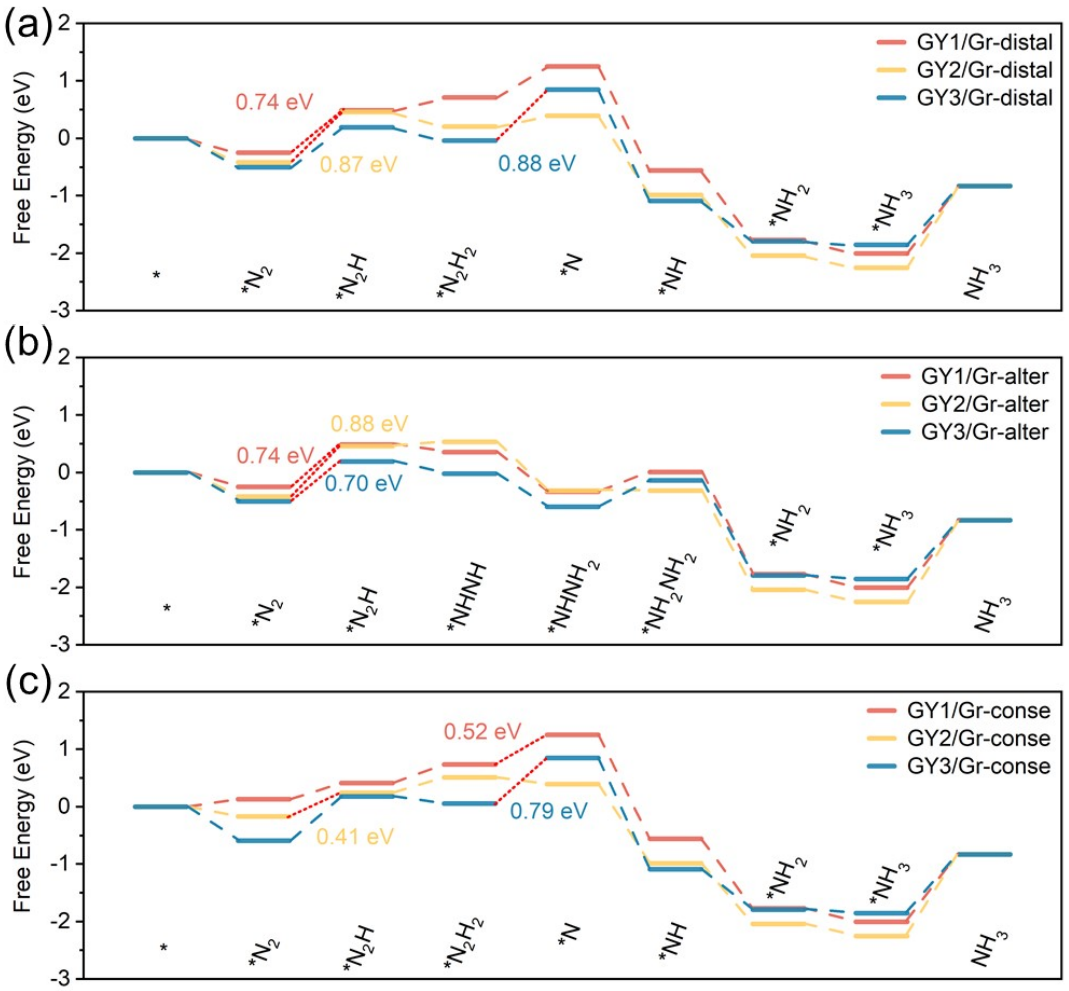

Fig. S4 NRR energy step diagrams of Ti@GY1/Gr, Ti@GY2/Gr and Ti@GY3/Gr for (a) distal, (b) alternating and (c) consecutive paths respectively.

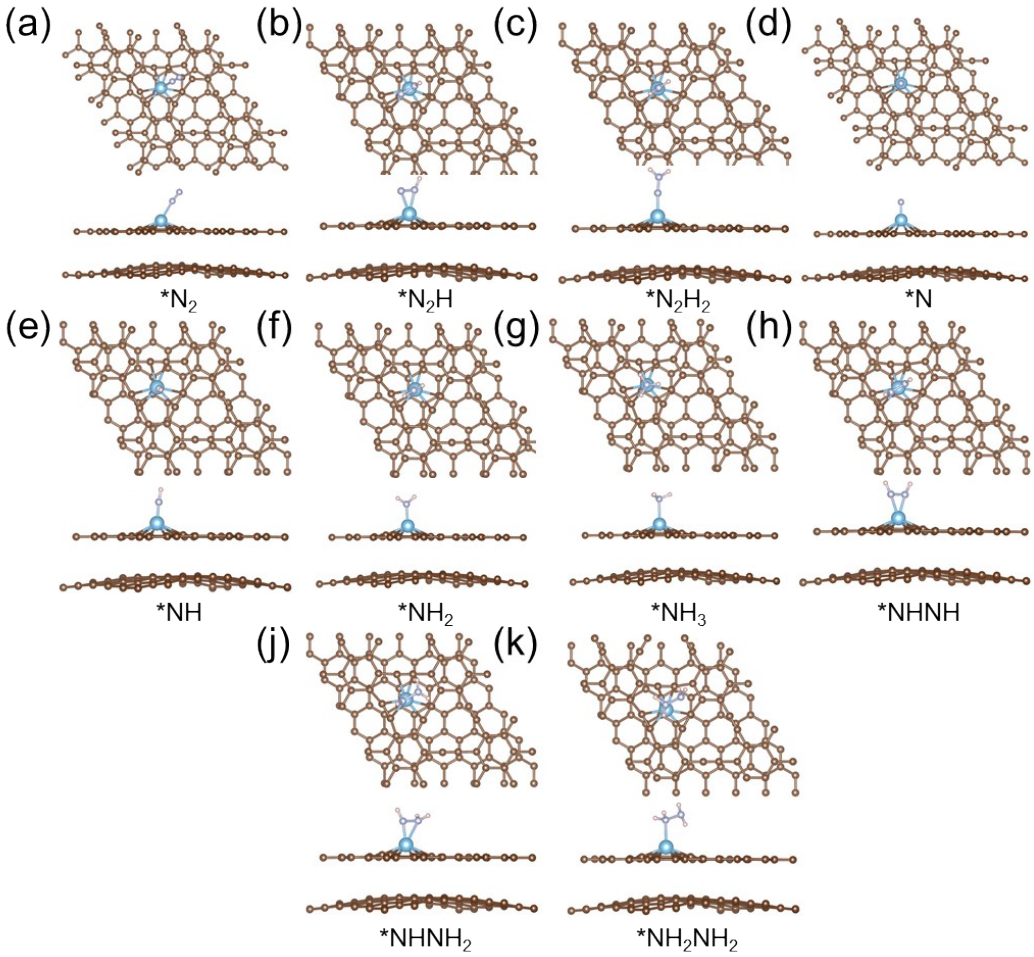

Fig. S5 Structure of all intermediates for distal and alternating paths on Ti@GY1/Gr.

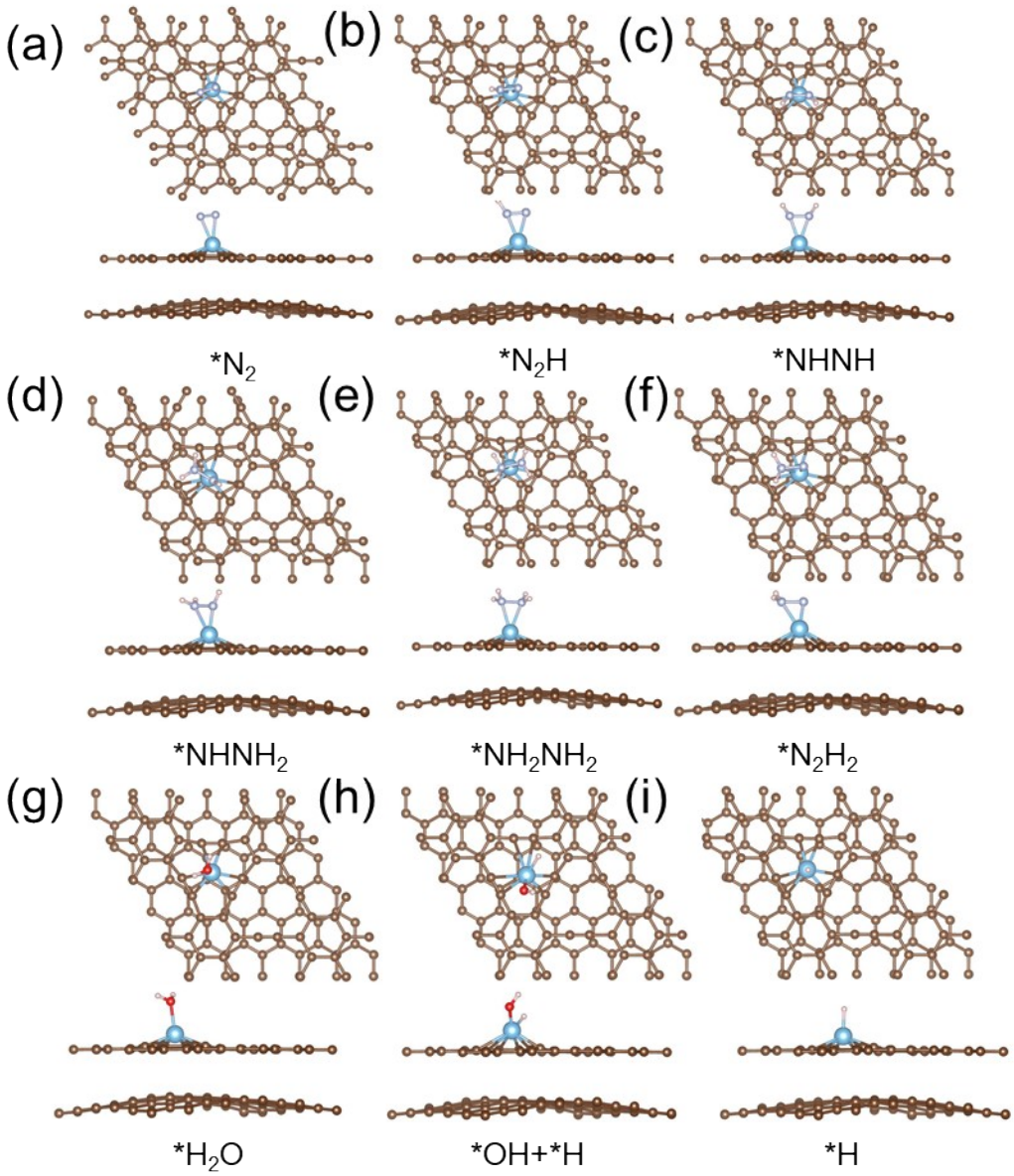

Fig. S6 Structure of all intermediates for consecutive, enzy and hydrogen evolution reaction paths on Ti@GY1/Gr.

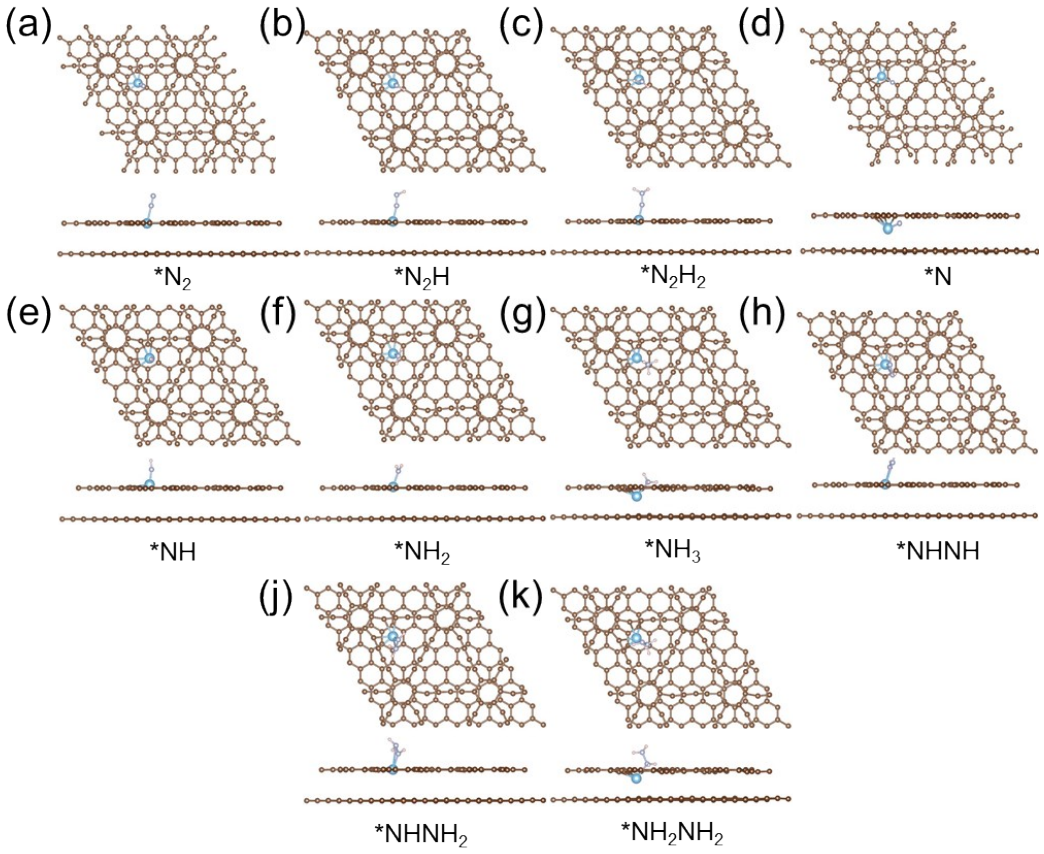

Fig. S7 Structure of all intermediates for distal and alternating paths on Ti@GY2/Gr.

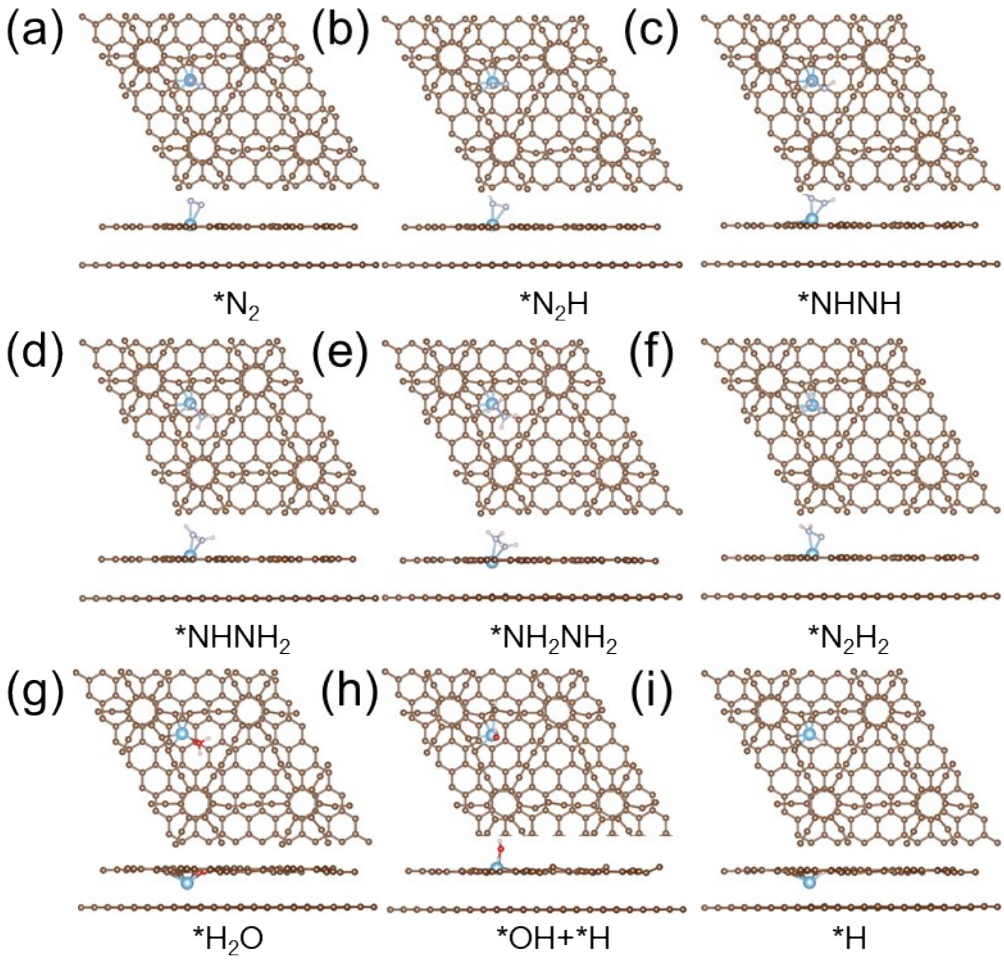

Fig. S8 Structure of all intermediates for consecutive, enzy and hydrogen evolution reaction paths on Ti@GY2/Gr.

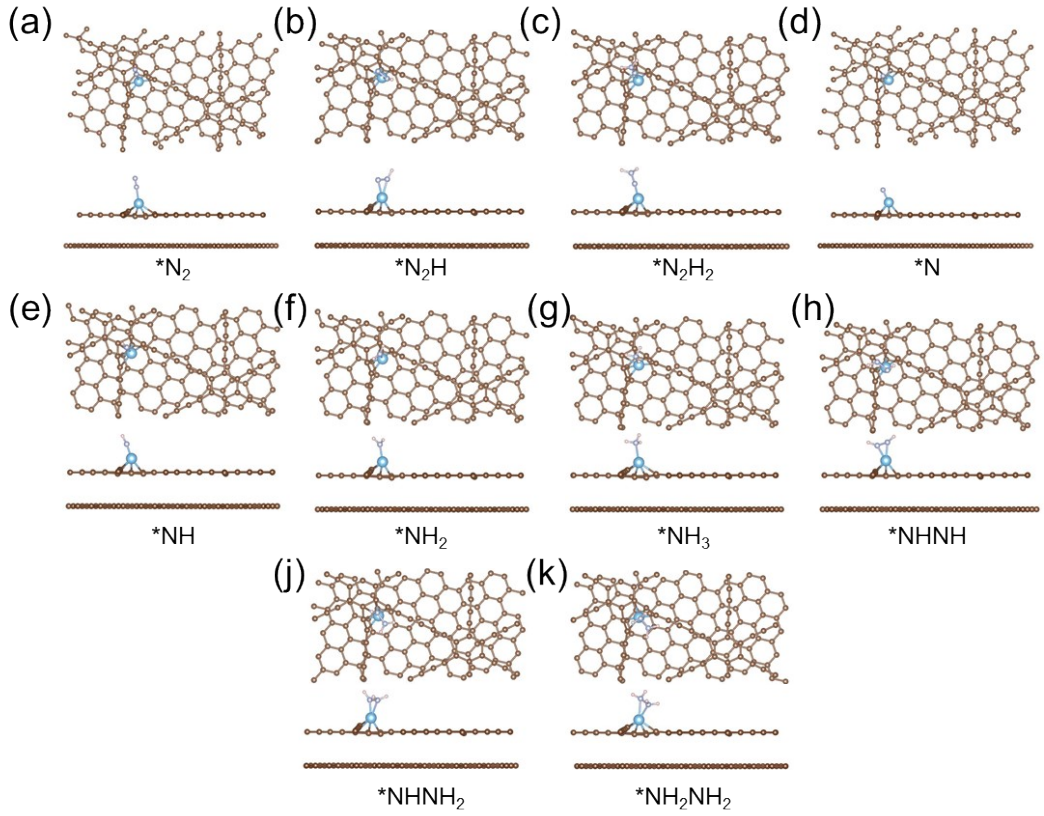

Fig. S9 Structure of all intermediates for distal and alternating paths on Ti@GY3/Gr.

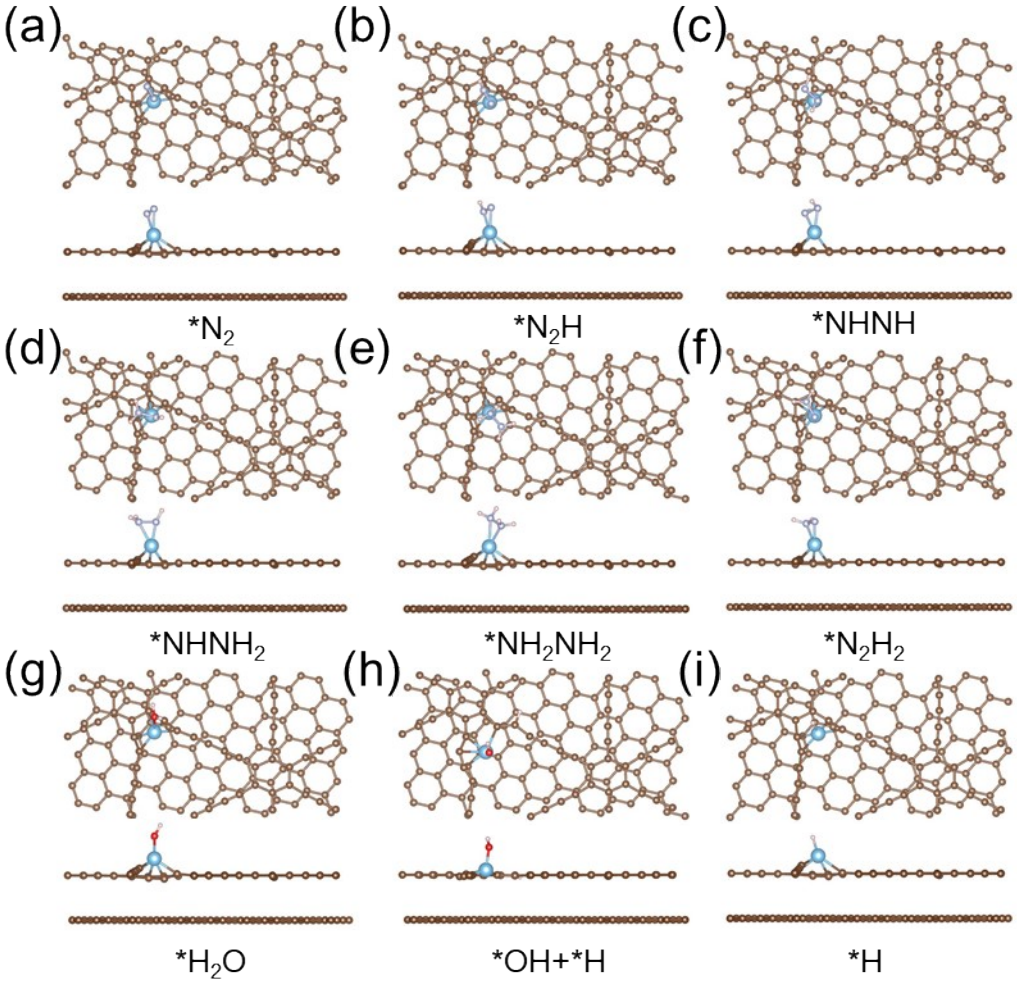

Fig. S10 Structure of all intermediates for consecutive, enzy and hydrogen evolution reaction paths on Ti@GY3/Gr.

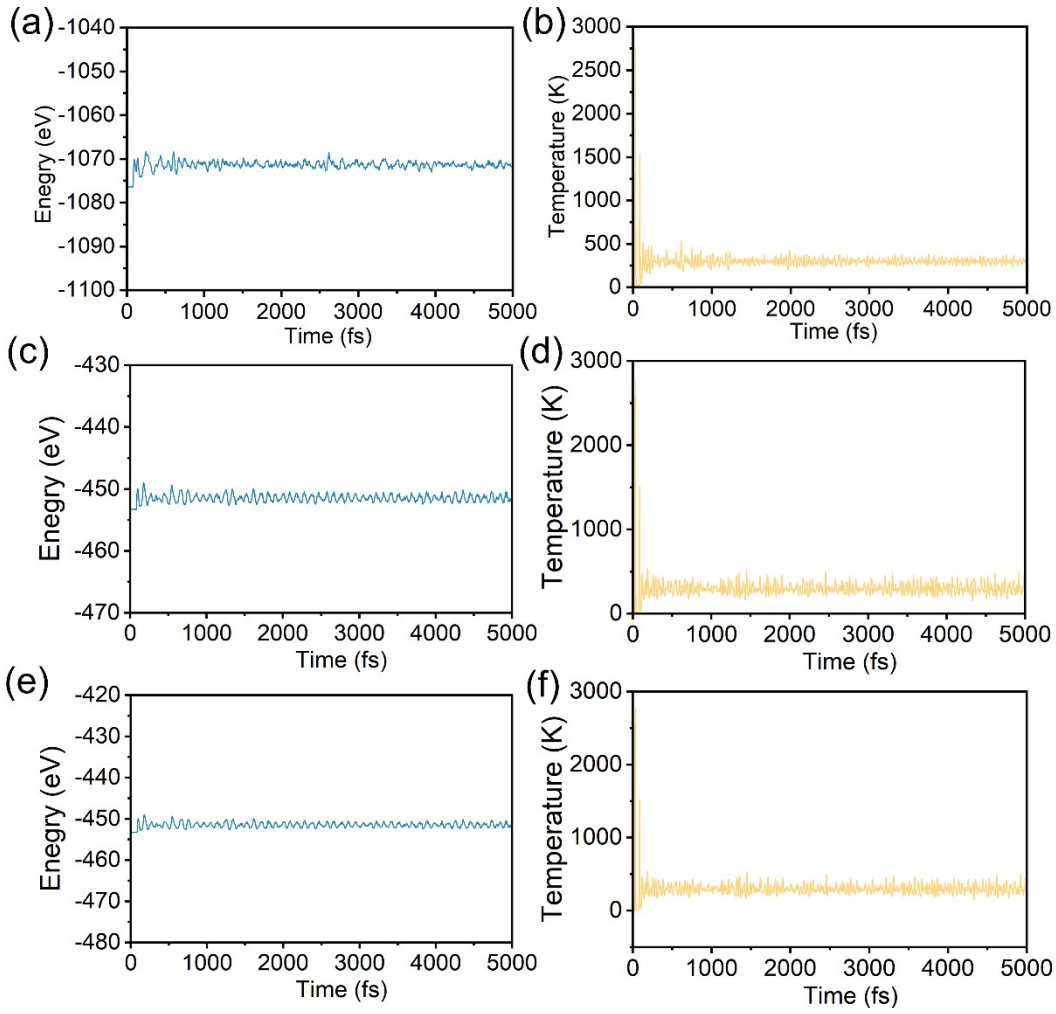

Fig. S11 (a, c, e) Energy and (b, d, f) temperature changes over time for AIMD simulation of Ti@GY1/Gr, Ti@GY2/Gr and Ti@GY3/Gr at 300 K.

References

1 G. Kresse and J. Hafner, *Phys. Rev. B*, 1993, **48**, 13115–13118.
2 G. Kresse and J. Hafner, *Phys. Rev. B*, 1993, **47**, 558–561.
3 G. Kresse and D. Joubert, *Phys. Rev. B*, 1999, **59**, 1758–1775.
4 J. P. Perdew and Y. Wang, *Phys. Rev. B*, 1992, **45**, 13244–13249.
5 J. P. Perdew, K. Burke and M. Ernzerhof, *Phys. Rev. Lett.*, 1996, **77**, 3865–3868.
6 S. Grimme, J. Antony, S. Ehrlich and H. Krieg, *J. Chem. Phys.*, 2010, **132**, 154104.
7 G. Makov and M. C. Payne, *Phys. Rev. B*, 1995, **51**, 4014–4022.
8 Noskov, J. K., Rossmeisl, J., Logadottir, A., Lindqvist, L., Kitchin, J. R., Bligaard, T., & Jonsson, H. J. Phys. Chem. B, 2004, 108, 17886–17892.
9 J. Rossmeisl, A. Logadottir and J. K. Nørskov, *Chem. Phys.*, 2005, **319**, 178–184.
10 V. Wang, N. Xu, J.-C. Liu, G. Tang and W.-T. Geng, *Comput. Phys. Commun.*, 2021, **267**, 108033.